

RESEARCH ARTICLE

# The processes of firebrand deposition and accumulation from wind-driven firebrand showers

Sayaka Suzuki<sup>1</sup>  | Samuel L. Manzello<sup>2</sup> 

<sup>1</sup>National Research Institute of Fire and Disaster (NRIFD), Chofu, Tokyo, Japan

<sup>2</sup>Reax Engineering, Berkeley, California, USA

## Correspondence

Sayaka Suzuki, National Research Institute of Fire and Disaster (NRIFD), Chofu, Tokyo, Japan.

Email: [sayakas@fri.go.jp](mailto:sayakas@fri.go.jp)

## Abstract

Firebrands, or smoldering and/or flaming particles, are in fact the main culprit to destroy structures in large outdoor fires. A recent comprehensive review of firebrand combustion reported that deposition and subsequent accumulation processes remain largely unexplored. As part of this work, a series of experiments were undertaken to investigate firebrand deposition and accumulation processes in the National Research Institute of Fire and Disaster (NRIFD)'s wind facility. A reduced-scale firebrand generator was utilized, and various flow obstructions were placed downstream of these firebrand generators to better understand these complex deposition processes. Results of these investigations for multiple wind speeds, firebrand size and mass distributions, and obstacle placement are presented and discussed.

## KEYWORDS

accumulation, deposition, firebrands, large outdoor fires, wind

## 1 | INTRODUCTION

Large outdoor fires are becoming commonplace in many countries (see Figure 1). Wildfires that spread into communities, referred to as wildland–urban interface (WUI) fires, are significant global problem, and one component of the large outdoor fire problem.<sup>1</sup> Over the past several years, WUI fires have been present in every continent.<sup>2</sup>

Urban fires and informal settlement fires are two other important aspects of the large outdoor fire problem. For example, China and Japan have experienced large urban fires.<sup>3</sup> Some after strong earthquakes, such as 1997 Hanshin-Awaji Earthquake, yet it is not a necessary condition for these urban fires to develop.

A major factor in both WUI and urban fire spread is firebrand production.<sup>4</sup> When structures burn in these fires, pieces of burning material, known as firebrands, are generated, become lofted, and are carried by the wind. This results in showers of wind-driven firebrands. A shower of firebrands ignites unburnt fuels, far from original fire location and starts new fires, labeled as spot fires. These spot fires overwhelm firefighting resources.<sup>1,4</sup>

In Japan, several city-fire spread models were developed for damage estimation. These models were based on past city fire damages and use empirical formula under limited situations.<sup>5</sup> There is

a lack of scientific and reliable data needed to advance such models further; especially for firebrand accumulation.

More than a decade ago, the state of California in the United States identified the need to develop an approach to harden communities to WUI fires exposure. The term harden simply indicates making infrastructure in communities more ignition resistant. The premise has its roots in the development of standards and codes developed to mitigate urban fire disasters that were observed in the United States, such as the 1871 Great Chicago Fire or 1904 Baltimore Fire. The urban fire codes and standards provide the basis for fire-resistant construction in many countries throughout the world. In the United States, the concept of WUI fire building codes and standards is far newer, due to the more recent WUI fire problem in this country.

Developing test standards for outdoor fire exposures presents significant challenges. Based on post-fire studies of ignition vulnerabilities in WUI fires, standard test methods were devised by the office of the State Fire Marshal (SFM) in California to address ignition vulnerabilities to exterior walls, exterior windows, horizontal projections such as eaves, decking assemblies, and the use of ignition resistant materials. It is important to note that the exposure conditions used in these test methods are best guess estimates of what exposure conditions would be in a WUI fire and were developed with the best available



**FIGURE 1** Great Meiriki Fire of 1657, Japan (top left), Great Chicago Fire of 1871, USA (top right), Lick Creek Fire of 2021, Oregon, USA (bottom left), Black Saturday 2009, Australia (Attribution: Richmeister at English Wikipedia) (bottom center), and Imizamo Yothu Informal Settlement Fires of 2017, South Africa (Credit: Aletta Harrison/GroundUp) (bottom right)

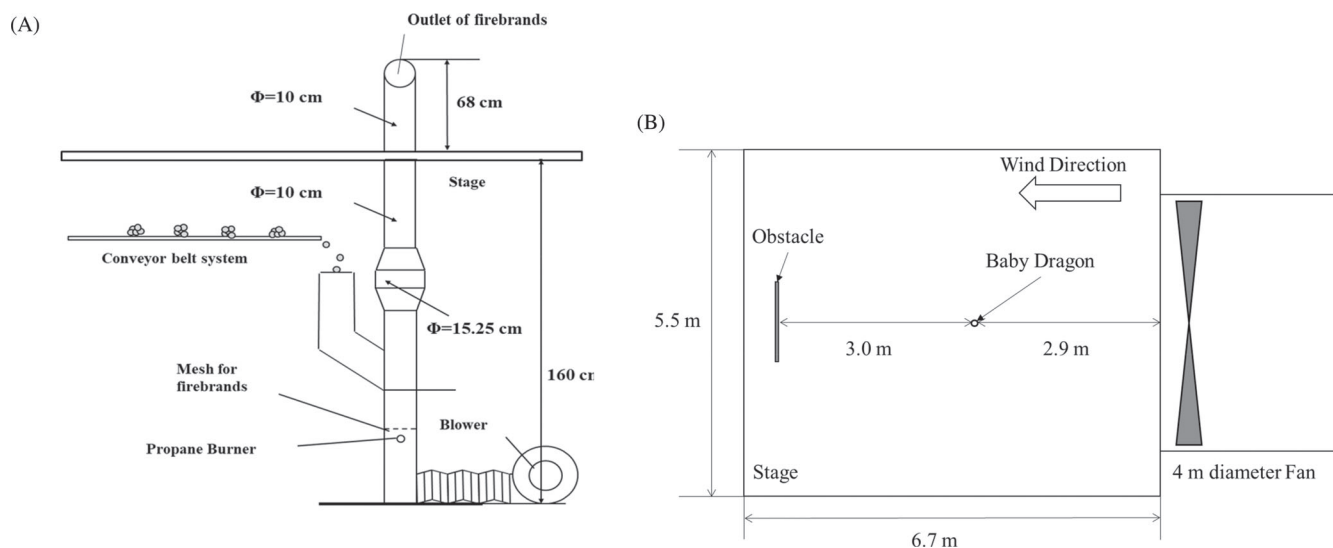


**FIGURE 2** (A) The reduced-scale firebrand generator is shown installed in NRIFD's wind facility. Wood pieces are continuously fed into the device to generate firebrand showers (B) NRIFD's wind facility layout

information at that time. For these reasons, it is not surprising WUI communities will continue to be lost in the future. The international standards organization (ISO) has just begun to address the large outdoor fire problem, as WUI fires are occurring all over the globe. Recently, ISO/TC92/WG14 has published ISO/TR4188:2022, "Large outdoor fires and the built environment—Global overview of different approaches to standardization" as a first step<sup>6</sup> and is in the process of developing ISO/DIS 6021 "Firebrand Generator".<sup>7</sup>

As structures are exposed to wind, stagnation planes are produced around structures. The authors demonstrated that firebrands may accumulate in these stagnation planes.<sup>8</sup> In a subsequent study performed by the authors,<sup>9</sup> a series of full-scale experiments revealed that wind speed influences not only the spatial location and extent of the accumulated firebrands in the stagnation plane in front of the obstacle but also the nature of the smoldering combustion intensity of the accumulated firebrands.

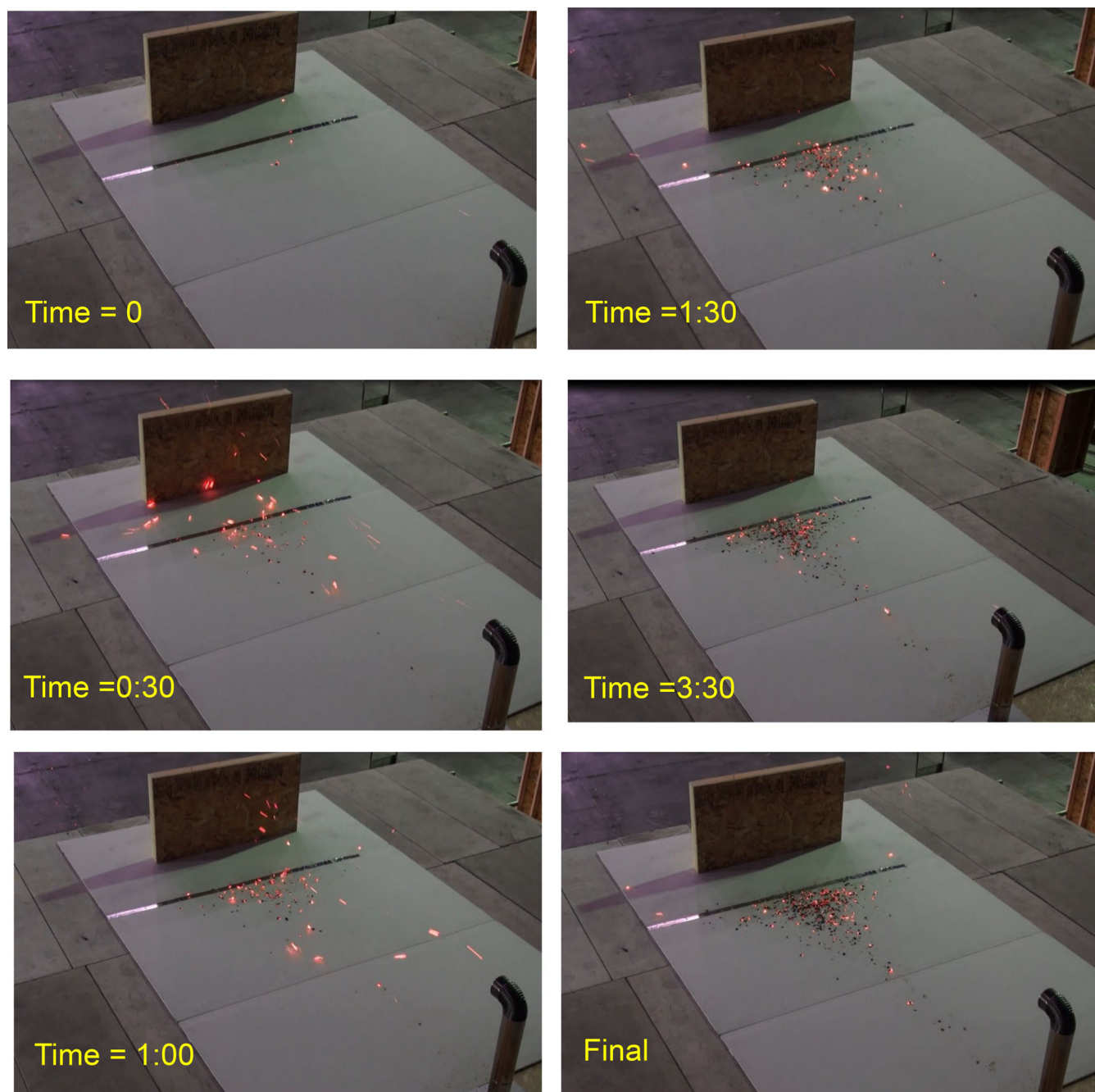


**FIGURE 3** Time lapse image of experiments with firebrands made from Japanese Cypress wood chips under 6 m/s wind

Some recent studies have also begun to look at firebrand deposition and accumulation processes using non-burning particles as surrogates for firebrands.<sup>10,11</sup> For example, studies have looked at firebrand deposition around an entire building, but the firebrands are not burning.<sup>10,11</sup> The lack of firebrand combustion is an important deficiency in these studies and there was no attempt to compare any results to those that include firebrand combustion. For example, during the combustion process, firebrands are often covered in sticky char formation, and this is not well represented by non-burning particles. In another study by a different group, firebrand combustion is considered, but it is a pure modeling study with no experimental validation.<sup>12</sup>

A comprehensive review of firebrand combustion reported that deposition and accumulation processes remain largely unexplored.<sup>4</sup> As a result, this paper describes an in-depth study of this phenomenon at a reduced scale to determine if useful insights may be obtained from simpler experiments. Full-scale experiments are useful, but these are very expensive, time-consuming, and depend on very expensive facilities. In this work, the authors have devised a much less expensive, simpler methodology to understand the complex processes of firebrand deposition and accumulation in front of obstacles. The firebrand distributions were varied to simulate both burning structures and vegetation, as prior studies were focused on vegetative firebrands.<sup>9,13</sup>



## 2 | EXPERIMENTAL DESCRIPTION

A reduced-scale continuous firebrand generator was used to generate firebrand showers (Figure 2A).<sup>14</sup> The overall schematic of

the experimental layout is shown in Figure 2B. The obstacle was placed downstream of the firebrand generator and the wind speed was varied at 4, 6, 8, and 9 m/s. Specifically, the obstacle used in this study had the dimensions of 660 cm (H) by 1275 cm (W) and was located at a distance of 3 m from the device to visualize the transport process shown in Figure 3.

The following experimental description follows those presented elsewhere.<sup>14</sup> The reduced-scale continuous-feed firebrand generator (baby Dragon) consisted of two parts: the main body and continuous feeding component. The capability of a smaller sized firebrand generator to develop continuous firebrand showers has been described. Japanese Cypress wood chips, which represent firebrands generated from structure combustion, and Douglas-fir wood pieces, which represent firebrands generated from vegetation combustion, were used to produce firebrands. The Japanese Cypress wood chips had dimensions of  $28 \text{ mm} \pm 7.5 \text{ mm}$  (L) by  $18 \text{ mm} \pm 6.3 \text{ mm}$  (W) by  $3 \text{ mm} \pm 0.8 \text{ mm}$  (H) (average  $\pm$  SD), respectively, before combustion. These were provided by a supplier and filtered to remove really small wood chips using a 1-cm mesh. Douglas-fir wood pieces were machined to dimensions of  $7.9 \text{ mm}$  (H) by  $7.9 \text{ mm}$  (W) by  $12.7 \text{ mm}$  (L). These sizes were selected based on research on firebrand generation from structures as well as vegetation.<sup>15–18</sup> In general, firebrands generated from structure combustion have larger projected area at a given mass and flatter shapes. Similar to the authors' prior full-scale studies, firebrands made from Japanese Cypress wood chips have approximately double the projected areas at a certain mass, compared with firebrands generated from Douglas-fir wood pieces as also seen in.<sup>19</sup> The difference in wind speeds on characteristics was not observed.

Figure 3 shows the time lapse images of experiments at 6 m/s with Japanese Cypress wood chips used as the feeding material. It can be observed that initially the accumulation area is not clear as there are not enough firebrands. More and more firebrands start depositing, leading to the eventual accumulated area as time progresses. After a certain period of time, the accumulated area does not change. This

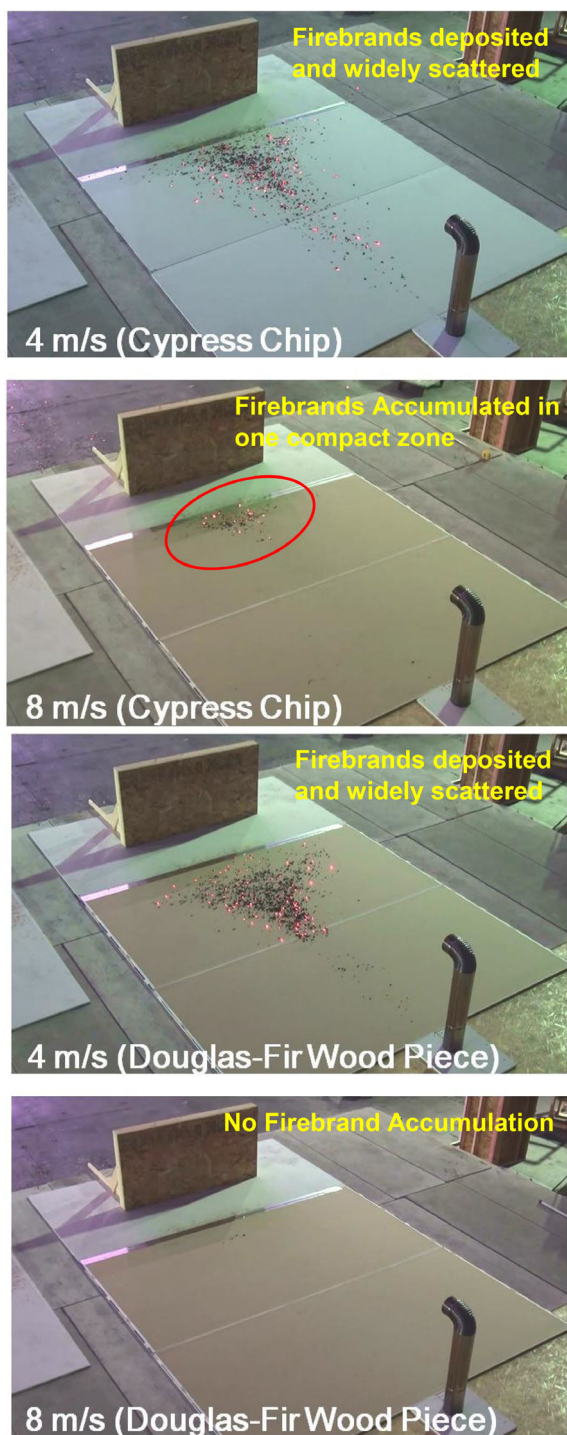


**FIGURE 4** Images of experiments with a 660 cm (H) by 1275 cm (W) obstacle under different wind speeds—4 and 8 m/s, with different feeding materials—Japanese Cypress wood chips and Douglas-fir wood pieces. Exactly 10 min of firebrand exposure has elapsed in these images

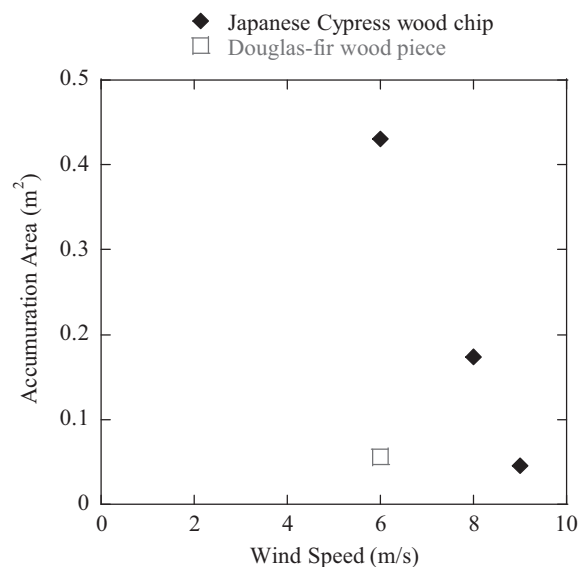


**FIGURE 5** Measured accumulated area for various wind speeds

phenomenon is the same as mentioned in reference.<sup>9</sup> Thus, the obstacle was exposed to firebrand showers for the same duration under different wind speeds.

### 3 | RESULTS AND DISCUSSION

#### 3.1 | COMPARISON OF ACCUMULATION PATTERNS

Figure 4 displays images of experiments with different wind speeds (4 and 8 m/s) and feeding materials (Japanese Cypress chips and Douglas-fir wood pieces). Images show that firebrands made from Japanese Cypress wood chips and from Douglas-fir wood pieces accumulated differently in front of the same obstacle.

During experiments with wind speed of 4 m/s, it was observed that firebrands were unable to accumulate into one compact zone, but were very scattered. As the wind speed increased, firebrands accumulated more in a compact zone. It was observed that firebrands made from Japanese Cypress wood chips managed to accumulate in front of the obstacle up to 9 m/s, while those made from Douglas-fir wood pieces did not accumulate under 8 and 9 m/s wind.

The accumulated area was measured using image processing software. Based on repeat measurements of different areas, the standard

uncertainty in determining the projected area was  $\pm 10\%$ . Figure 5 displays the measured area of the accumulated firebrands as a function of wind speed. In the case of 4 m/s wind, as firebrands made from both Japanese Cypress wood chips and Douglas-fir wood pieces did not accumulate as shown in Figure 4, those were not considered “accumulation” nor included in Figure 5. Firebrands made from Douglas-fir wood pieces did not accumulate under 8 and 9 m/s wind as shown in Figure 4, those data are also not included in Figure 5. As the wind speed increased, the area of accumulated firebrands reduced significantly. For experiments with firebrands made from Douglas-fir wood pieces under 8 and 9 m/s, no accumulation zone was observed. It is clear in Figure 5 that firebrands from Douglas-fir wood pieces accumulated to smaller areas than those from Japanese Cypress wood chips. Comparison was made in order to investigate the difference in accumulation behaviors of firebrands. It suggests that the difference in firebrand characteristics has an effect on the accumulation behavior of firebrands in front of wall assemblies.

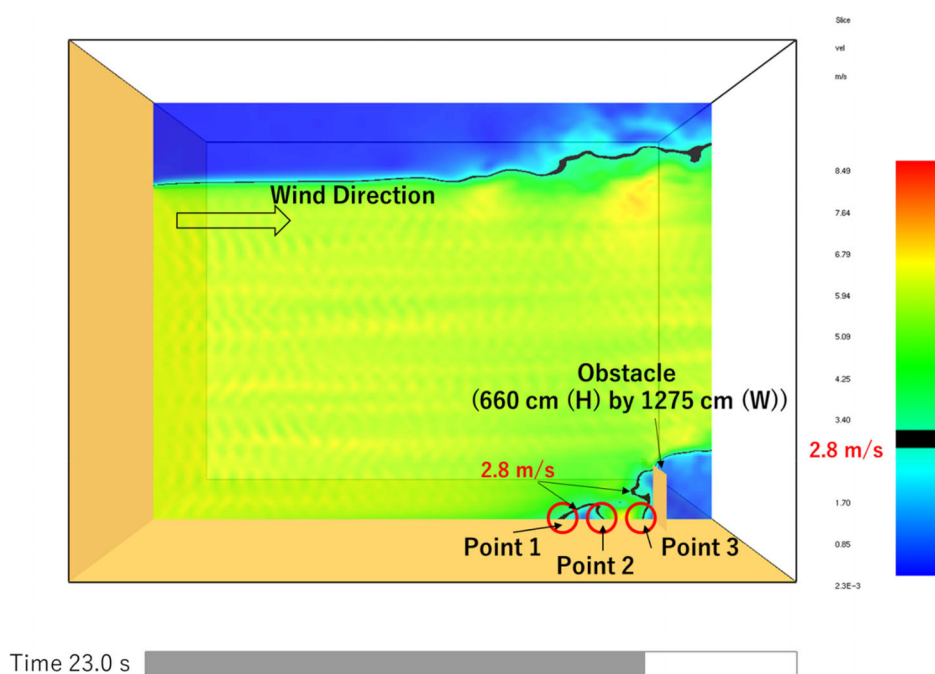
#### 3.2 | COMPARISON WITH WIND PROFILE AROUND THE OBSTACLES

In order to understand how firebrands transport with wind, the National Research Institute of Fire and Disaster (NRIFD) wind facility

**TABLE 1** Calculation of  $v$ , the upper limit of wind speed on a firebrand allowing firebrands to stay in the same place based on mass and projected area of a firebrand

	Projected area of a firebrand [cm <sup>2</sup> ]	Mass of a firebrand [g]	$v$ [m/s]
Douglas-fir wood pieces	0.78	0.05	2.3
Japanese Cypress wood chips	1	0.03	1.6
Japanese Cypress wood chips	1	0.1	2.8

**FIGURE 6** FDS simulation under 6 m/s inlet wind speed. The black lines show zones of wind speed of 2.8 m/s. There are three locations where these zones occurred in front of the obstacle for an inlet wind speed of 6 m/s



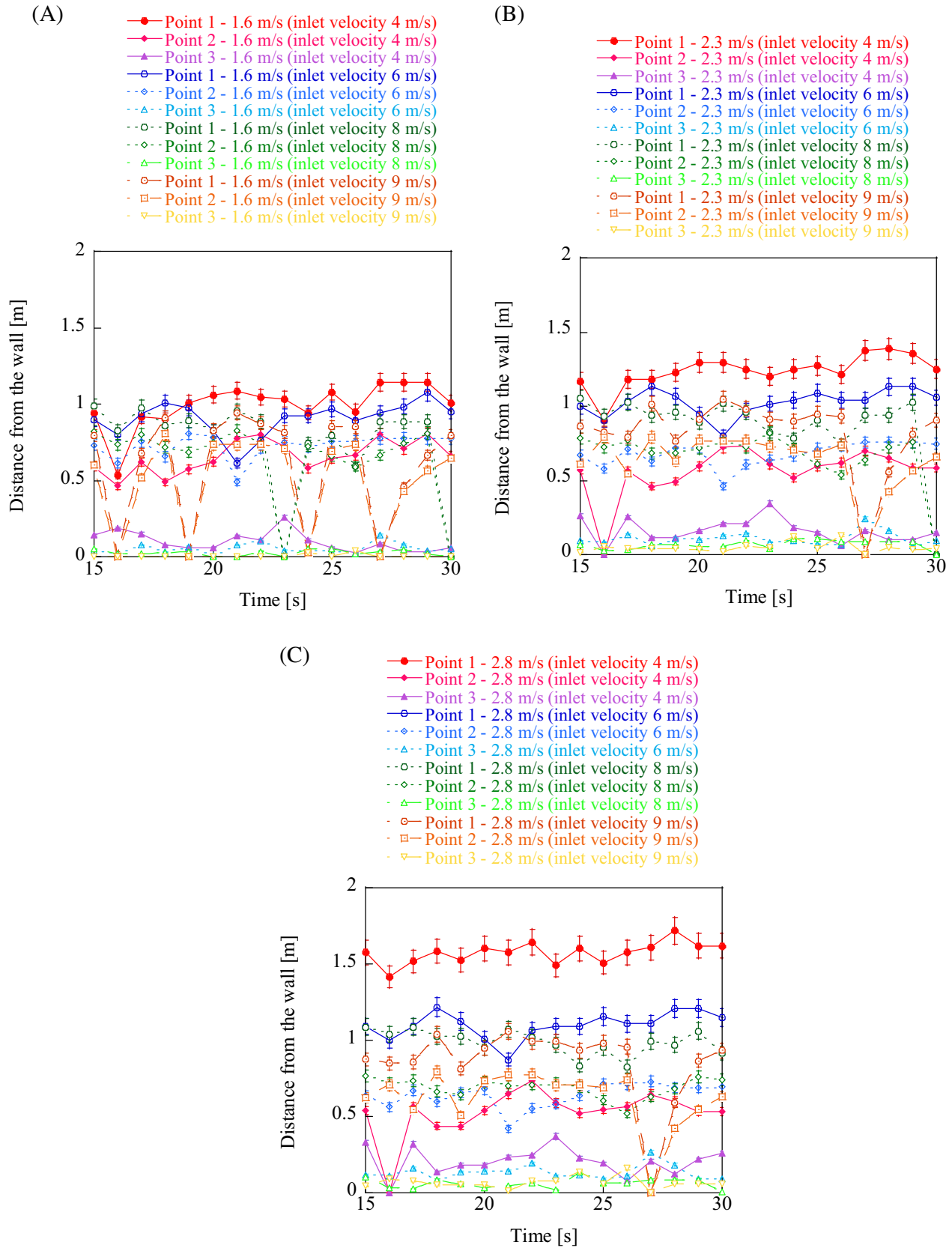


**FIGURE 7** (A–C) shows the results of the simulations for various inlet wind speeds and locations where zones of 1.6, 2.3, and 2.8 m/s, were predicted to occur with respect to distance from the flow obstacle

and the wind profile around the obstacle was simulated by using Fire Dynamic Simulator (FDS).<sup>20</sup> The dimension was 6.7 m (L) × 5.4 m (W) × 5 m with 1 grid 5 cm × 5 cm × 5 cm. The grid sizes were intentionally selected in this size range, as the range of flow patterns is expected in this range. The obstacle was placed at 6 m from the fan as described in Figure 2B. Assuming the firebrands are mostly transported by the wind, but once firebrands fall on the ground, it was observed that firebrands moved on the ground along with wind until they stop due to the friction. Based on previous work,<sup>9</sup> though many factors have to be considered in order to understand firebrand accumulation in front of the obstacles, a very basic, first-step analysis was conducted to try to understand the observed results. In order for firebrands to accumulate, the force by wind on a firebrand ( $F_{\text{wind}}$ ) should be balanced with the friction force between the firebrand and the floor (gypsum board) ( $F_{\text{friction}}$ ).

$$F_{\text{friction}} = F_{\text{wind}} \quad (1)$$

Here,

$$F_{\text{friction}} = \mu m_{\text{firebrand}} g \quad (2)$$

$$F_{\text{wind}} = \frac{1}{2} \rho_{\text{air}} v^2 \times A \quad (3)$$

- Location of the closest point of the accumulation zone to the obstacle in experiments with firebrands made from Douglas-fir wood pieces
- ◆— Location of the closest point of the accumulation zone to the obstacle in experiments with firebrands made from Japanese Cypress wood chips
- ▲— Location of Point 2 in FDS simulation ( $u_f = 2.3$  m/s)
- Location of Point 2 in FDS simulation ( $u_f = 2.8$  m/s)
- Location of the furthest point of the accumulation zone to the obstacle in experiments with firebrands made from Douglas-fir wood pieces
- ◇— Location of the furthest point of the accumulation zone to the obstacle in experiments with firebrands made from Japanese Cypress wood chips
- △— Location of Point 1 in FDS simulation ( $u_f = 2.3$  m/s)
- Location of Point 1 in FDS simulation ( $u_f = 2.8$  m/s)

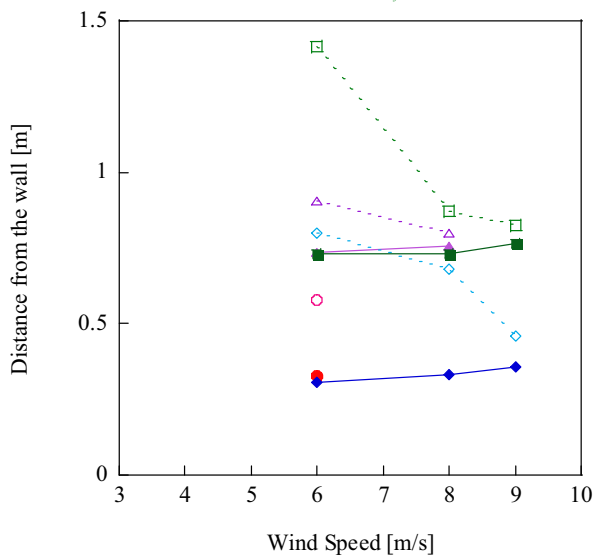


**FIGURE 8** Comparison of location of firebrand accumulation points in experiments with respect to FDS simulations of velocity zones of 2.3 and 2.8 m/s

Therefore,  $\mu$  is the friction coefficient between a gypsum board and smoldering firebrands,  $m_{\text{firebrand}}$  is the average mass of a firebrand [kg],  $\rho_{\text{air}}$  is the density of the air [kg/m<sup>3</sup>],  $g$  is gravitation acceleration [m/s<sup>2</sup>],  $v$  is wind speed on a firebrand [m/s], and  $A$  is the average projected area of a firebrand [m<sup>2</sup>].

$$\mu m_{\text{firebrand}} g = \frac{1}{2} \rho_{\text{air}} v^2 \times A \quad (4)$$

The value  $v = 2.3$  m/s was calculated for firebrands from Douglas-fir wood pieces; this means that the flow in front of obstacles allows firebrands to stay in the same place if the flow around firebrands is under 2.3 m/s<sup>9</sup> (upper limit of wind speed). Using the same formula developed above from reference,<sup>9</sup> the value  $v$  was calculated to be 1.6 m/s for firebrands from Japanese Cypress chips. All information for calculation is provided in Table 1.

As stated before, Japanese Cypress chips have more variety in size and mass combination compared with Douglas-fir wood pieces. Here, Japanese Cypress chips are used to produce firebrands similar to that from structure combustion. As a result, the corresponding firebrands produced from Japanese Cypress chips produced a greater variety of firebrands in size and mass. Given that  $v$  was calculated based on the average mass and projected area combination, it is also important to understand that  $v$  also may have a range of values. Based on the analysis in reference,<sup>9</sup>  $v$  could go up to 5 m/s (for heavy or small projected area firebrands) or go down to near 1 (for light firebrands) with different combinations of mass and projected area. These variabilities make the locations different for the accumulation pattern from firebrands as compared with the more uniform Douglas-fir wood pieces. Accordingly, for Japanese Cypress wood chips, two different wind speeds were considered where firebrands may remain in front of obstacles. This was done by assuming a combination of 0.1 g and

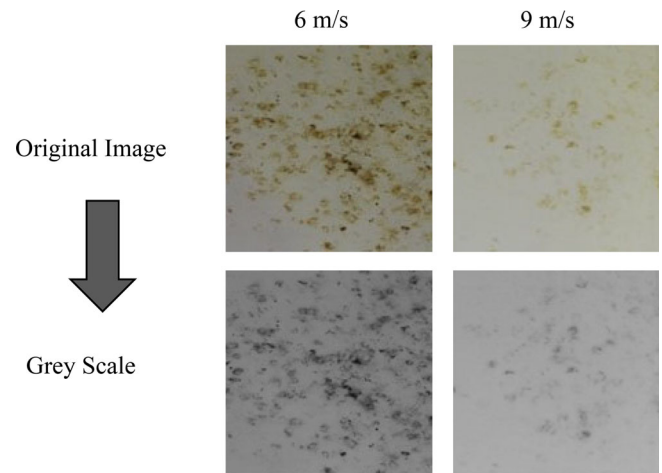


**FIGURE 9** Accumulated firebrands swept off after the completion of the experiments. Ignition points of the gypsum board paper are observed at 6 m/s but not 9 m/s. Japanese Cypress wood chips were used to simulate structure firebrands. The top images were original. The bottom images were grey scaled

1 cm<sup>2</sup> projected area, then  $v$  can be calculated to be 2.8 m/s. This is higher than the velocity for Douglas-fir wood pieces. As a result, these three wind speeds, or 1.6, 2.3, and 2.8 m/s were considered to observe the velocity zone around the obstacles in FDS simulation.

Figure 6 shows an FDS simulation under 6 m/s inlet wind speed. The black lines show zones of wind speed of 2.8 m/s. There are three locations where these zones occurred in front of the obstacle for an inlet wind speed of 6 m/s. From the experimental observations, firebrands were mainly observed to accumulate between Point 1 and Point 2, as the predicted velocity profiles in these regions were less than the threshold value of 2.8 m/s. Point 1 was defined as the furthest location, Point 2 was defined as the middle location, and Point 3 was defined as the nearest location to the obstacle. The simulations are only shown for an inlet velocity of 6 m/s, but for inlet velocities of 4, 8, and 9 m/s, similar Point 1, Point 2, and Point 3 were also predicted.

Figure 7A–C shows the results of the simulations for various inlet wind speeds and locations where zones of 1.6, 2.3, and 2.8 m/s were predicted to occur with respect to distance from the obstacle. In general, the distance that these three flow zones were predicted to occur from the wall increased as the wind speed decreased, for a given  $v$  increase. As shown in Figure 7A–C, all three points indicate 0 m occasionally, which means there are no predicted locations less than  $v$  at the ground level. This behavior occurs more often at higher wind speed and at lower  $v$ . As such, lower  $v$  would result in no accumulation zones at higher wind speed.

Figure 8 shows the locations of Point 1 and Point 2, compared with the experimental results. From FDS simulations, it is expected that firebrands may stay at locations between Point 1 and Point 2, as the wind speeds are less than  $v$ . Comparison shows a general agreement with experimental results and FDS observations. The firebrands made from Douglas-fir wood pieces are more difficult to accumulate than firebrands made from Japanese Cypress wood chips, and as the wind speed increased, the firebrand accumulation zone became smaller. The location of Point 2 is similar for firebrands made from Douglas-fir wood pieces and firebrands made from Japanese Cypress wood chips. For

details, the locations of Point 1, corresponding to the furthest point of firebrand accumulation zone from the obstacle in experiments, and Point 2, corresponding to the nearest point of firebrand accumulation zone from the obstacle in experiments, in FDS simulations, are 1.5 to 2 times further than experimental results. One of the reasons could be the unknown friction coefficient, which was assumed to be 0.5 based on the friction coefficient between wood.<sup>21</sup> This may be different between paper and a firebrand made from Japanese Cypress wood chips, and between paper and a firebrand made from Douglas-fir wood pieces. In addition, the FDS simulations for this study considered only the wind profile. As such, the current simulation ignores the localized wind profiles around an individual firebrand after accumulation. This may be another reason for the differences.

### 3.3 | HEAT FEEDBACK TO GYPSUM BOARDS

When firebrands accumulate into compact zones, it is known that they may provide sufficient heat feedback to ignite materials.<sup>9</sup> In full-scale experiments,<sup>9</sup> when firebrands were observed to accumulate into compact zones in front of obstacles, the paper of the gypsum board was observed to ignite due to accumulated firebrands. Figure 9 (top) displays images of the gypsum board surfaces after firebrands have been swept away. In the top (left) image, the wind speed was 6 m/s and several ignition points were observed. At 9 m/s, it may be seen that, since the firebrands were unable to accumulate into compact zones, sufficient heat feedback was not provided to ignite the gypsum board. This is similar behavior to the full-scale experiments despite the results from firebrands made from Douglas-fir wood pieces.<sup>9</sup> The intense ignition points were observed in experiments with 6 m/s wind, while the ignition points were observed to be less under higher wind speed.

An interesting observation was that the accumulated firebrands were able to ignite the gypsum board under certain conditions. It is

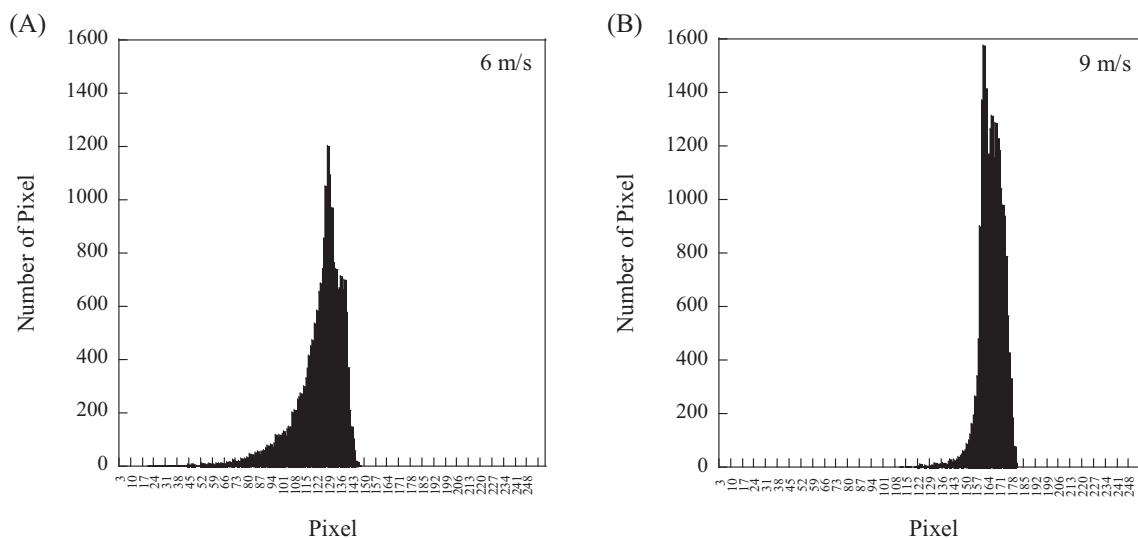


**FIGURE 10** Histogram based on grey scaled image in Figure 6 (bottom). (a) 6 m/s, (b) 9 m/s



well known that when using radiant heat in the presence of a spark (piloted ignition source), gypsum board will sustain flaming ignition for applied heat flux levels of 20 kW/m<sup>2</sup> or greater.<sup>22</sup> In the case of firebrands, Manzello et al.<sup>23</sup> calculated that the heat flux generated from an individual firebrand varied from 23.4 kW/m<sup>2</sup> for an applied airflow of 1.3 m/s and increased to 34.2 kW/m<sup>2</sup> for an applied airflow of 2.4 m/s. In the present work, it is estimated that firebrands will accumulate in front of the obstacles within velocity ranges of 1.6 or 2.8 m/s, for Japanese Cypress firebrands, and 2.3 m/s for Douglas-fir firebrands. For the gypsum board paper surface to ignite, it is clear that accumulated firebrands are capable of producing heat flux levels of 20 kW/m<sup>2</sup> or greater. Once the firebrands accumulate into compact zones, the arrival of additional firebrands serves to act as piloted ignition source. While there has been work in the literature to measure heat fluxes from firebrand piles, the authors of those studies indicated those measurement techniques will not work in realistic settings, such as the present experiments. The development of measurement techniques to quantify heat fluxes from realistic-scale experiments is required.

Both images were grey scaled (Figure 9 [bottom]), then pixels were counted by using image software in order to investigate the difference in the burn patterns. Figure 10A, B shows the peak under 9 m/s is higher than the peak under 6 m/s, which means that there were more ignition spots under 6 m/s as compared with 9 m/s. The histogram was steeper for 9 m/s cases than for 6 m/s cases and the number of lower pixels decreased more gently for 6 m/s. The findings indicated the ignition spots were darker, suggesting more intense combustion under 6 m/s than 9 m/s.

Future consideration will be needed to incorporate firebrands into future simulations, as selection of firebrand size and characteristics are of importance when considering the accumulation. In particular, to better aid understanding, the complex combustion processes of firebrands should be considered as part of future FDS development efforts.

## 4 | SUMMARY

A series of reduced-scale experiments were performed in order to investigate firebrand deposition and accumulation in front of an obstacle using Japanese Cypress wood chips and Douglas-fir wood pieces. For a specified wind speed, it was found that the characteristics of firebrands have an effect on accumulation behavior of firebrands in front of an obstacle. Firebrands made from Japanese Cypress chips were able to accumulate into one compact zone under wind speeds from 6 to 9 m/s, while those made from Douglas-fir wood pieces were able to accumulate into one compact zone under only 6 m/s wind. Important qualitative similarities between the full-scale and reduced-scale firebrand studies are that increased wind speed resulted: (1) decreased firebrand accumulation areas (2) less ignition points on gypsum board surfaces. Detailed investigation will be needed in the future for different obstacles placed downwind from the firebrand generator, as well as

further full-scale experiments generating firebrands similar to structure production for comparison. In addition, the authors plan to quantitatively measure the heat flux profiles imparted onto the surface under various experimental conditions. Methods to quantify heat flux profiles have been proposed and reviewed in the literature, but it is not clear if these indeed work in more realistic experimental settings presented here.

## CONFLICT OF INTEREST

The authors declare no conflict of interest.

## DATA AVAILABILITY STATEMENT

The data that support the findings of this study are available from the corresponding author upon reasonable request.

## ORCID

Sayaka Suzuki  <https://orcid.org/0000-0002-6635-5512>

Samuel L. Manzello  <https://orcid.org/0000-0002-3171-7333>

## REFERENCES

- Manzello SL, Almand K, Guillaume E, Vallerent S, Hameury S, Hakkarainen T. FORUM position paper. *Fire Saf J*. 2018;100:64-66. doi:[10.1016/j.firesaf.2018.07.003](https://doi.org/10.1016/j.firesaf.2018.07.003)
- Manzello SL, Blanchi R, Gollner MJ, et al. Summary of workshop large outdoor fires and the built environment. *Fire Saf J*. 2018;100:76-92. doi:[10.1016/j.firesaf.2018.07.002](https://doi.org/10.1016/j.firesaf.2018.07.002)
- Wang Y, Wadhvani R, Suzuki S, et al. Case studies of large outdoor fires involving evacuations. *Emergency Management & Evacuation (EME) Subgroup, Large Outdoor Fires & the Built Environment (LOF&BE) Working Group of the International Association for Fire Safety Science*. Zenodo; 2022. doi:[10.5281/zenodo.6544760](https://doi.org/10.5281/zenodo.6544760)
- Manzello SL, Suzuki S, Gollner MJ, Fernandez-Pello AC. Role of firebrand combustion in large outdoor fire spread. *Prog Energy Combust Sci*. 2020;76:100801. doi:[10.1016/j.pecs.2019.100801](https://doi.org/10.1016/j.pecs.2019.100801)
- Andoh S. Study on fire damage mitigation using simulation tools of urban fire spread and fire brigade operation, Master, Tokyo University of Science; 2014.
- ISO, Large outdoor fires and the built environment—Global overview of different approaches to standardization, ISO/TR 24188:2022. 2022.
- ISO, Firebrand generator, ISO/DIS 6021. <https://www.iso.org/standard/81912.html>.
- Manzello SL, Park S-H, Suzuki S, Shields JR, Hayashi Y. Experimental investigation of structure vulnerabilities to firebrand showers. *Fire Saf J*. 2011;46(8):568-578. doi:[10.1016/j.firesaf.2011.09.003](https://doi.org/10.1016/j.firesaf.2011.09.003)
- Suzuki S, Manzello SL. Experimental investigation of firebrand accumulation zones in front of obstacles. *Fire Saf J*. 2017;94:1-7. doi:[10.1016/j.firesaf.2017.08.007](https://doi.org/10.1016/j.firesaf.2017.08.007)
- Nguyen D, Kaye NB. Experimental investigation of rooftop hotspots during wildfire ember storms. *Fire Saf J*. 2021;125:103445. doi:[10.1016/j.firesaf.2021.103445](https://doi.org/10.1016/j.firesaf.2021.103445)
- Nguyen D, Kaye NB. Quantification of ember accumulation on the rooftops of isolated buildings in an ember storm. *Fire Saf J*. 2022;128:103525. doi:[10.1016/j.firesaf.2022.103525](https://doi.org/10.1016/j.firesaf.2022.103525)
- Mankame A, Shotorban B. Deposition characteristics of firebrands on and around rectangular cubic structures. *Front Mech Eng*. 2021;7:640979. doi:[10.3389/fmech.2021.640979](https://doi.org/10.3389/fmech.2021.640979)
- Suzuki S, Manzello SL. Investigating the effect of structure to structure separation distance on firebrand accumulation. *Front Mech Eng*. 2021;6:628510. doi:[10.3389/fmech.2020.628510](https://doi.org/10.3389/fmech.2020.628510)

14. Suzuki S, Manzello SL. Experiments to provide the scientific-basis for laboratory standard test methods for firebrand exposure. *Fire Saf J*. 2017;91:784-790. doi:[10.1016/j.firesaf.2017.03.055](https://doi.org/10.1016/j.firesaf.2017.03.055)
15. Suzuki S, Manzello SL, Hayashi Y. The size and mass distribution of firebrands collected from ignited building components exposed to wind. *Proc Combust Inst*. 2013;34(2):2479-2485. doi:[10.1016/j.proci.2012.06.061](https://doi.org/10.1016/j.proci.2012.06.061)
16. Manzello SL, Suzuki S. Generating wind-driven firebrand showers characteristic of burning structures. *Proc Combust Inst*. 2015;36(2):3247-3252. doi:[10.1016/j.proci.2016.07.009](https://doi.org/10.1016/j.proci.2016.07.009)
17. Suzuki S, Manzello SL. Firebrand production from building components fitted with siding treatments. *Fire Saf J*. 2016;80:64-70. doi:[10.1016/j.firesaf.2016.01.004](https://doi.org/10.1016/j.firesaf.2016.01.004)
18. Manzello SL, Maranghides A, Shields JR, Mell WE, Hayashi Y, Nii D. Mass and size distribution of firebrands generated from burning Korean pine (*Pinus koraiensis*) trees. *Fire Mater*. 2009;33(1):21-31. doi:[10.1002/fam.977](https://doi.org/10.1002/fam.977)
19. Suzuki S, Manzello SL. On unraveling community ignition processes: joint influences of firebrand showers and radiant heat applied to fuel beds. *Combust Sci Technol*. 2022;1-14. doi:[10.1080/00102202.2021.2019238](https://doi.org/10.1080/00102202.2021.2019238)
20. McGrattan KB, Hostikka S, McDermott R. *Fire Dynamics Simulator User's Guide (FDS Version 6)*. National Institute of Standards and Technology (NIST); 2017. doi:[10.6028/NIST.SP.1019](https://doi.org/10.6028/NIST.SP.1019)
21. Japanese Society of Mechanical Engineers, Ed. *JSME Mechanical Engineers' Handbook, Alpha 2*. Maruzen; 2014.
22. Dietenberger MA. *Ignitability of materials in transitional heating regimes*. Wood & fire safety: proceedings, 5th international scientific conference, April 18-22, 2004. Slovak Republic. [Svolen, Slovakia]: Faculty of Wood Sciences and Technology, Technical University of Zvolen, 2004:31-41.
23. Manzello SL, Park S-H, Cleary TG. Investigation on the ability of glowing firebrands deposited within crevices to ignite common building materials. *Fire Saf J*. 2009;44(6):894-900. doi:[10.1016/j.firesaf.2009.05.001](https://doi.org/10.1016/j.firesaf.2009.05.001)

**How to cite this article:** Suzuki S, Manzello SL. The processes of firebrand deposition and accumulation from wind-driven firebrand showers. *Fire and Materials*. 2022;1-10. doi:[10.1002/fam.3125](https://doi.org/10.1002/fam.3125)